

Received July 9, 2020, accepted July 19, 2020, date of publication July 22, 2020, date of current version August 4, 2020.

Digital Object Identifier 10.1109/ACCESS.2020.3011109

An Unmanned Intelligent Transportation Scheduling System for Open-Pit Mine Vehicles Based on 5G and Big Data

SAI ZHANG^{1,2}, CAIWU LU^{1,2}, SONG JIANG^{1,2}, LU SHAN³,
AND NEAL NAI XUE XIONG⁴, (Senior Member, IEEE)

¹School of Management, Xi'an University of Architecture and Technology, Shaanxi 710055, China

²School of Resources Engineering, Xi'an University of Architecture and Technology, Shaanxi 710055, China

³School of Business, The Hong Kong University of Science and Technology, Hong Kong


⁴Department of Mathematics and Computer Science, Northeastern State University, Tahlequah, OK 74464, USA

Corresponding authors: Sai Zhang (zhangsai168@126.com) and Caiwu Lu (lucaiwu@126.com)

This work was supported in part by the Natural Science Foundation of China, title: "Research on Intelligent Fusion and situation assessment of multi-source heterogeneous flow data of rock failure in underground metal mines", under Grant 51974223, title: "Research on 5D refined mining production scheduling model and collaborative optimization method in metal open pit under constraints of Grade-Price-Cost", under Grant 51774228, and title: "Experimental theory and method of time-varying calculation for fully mechanized mining process under artificial system environment in Yushen mining area", under Grant 51864046, and in part by the Natural Science Foundation of Shaanxi Province, title: "Research and development of key technologies for intelligent production control and intelligent decision-making of open pit coal mine under cloud service", under Grant 2019JLP-16, and title: "Integrated intelligent scheduling model of driverless multi vehicle cooperation in metal open pit under time and space road conditions, under Grant 2020JC-44.

ABSTRACT With the maturity of the Internet of Things, 5G communication, big data and artificial intelligence technologies, open-pit mine intelligent transportation systems based on unmanned vehicles has become a trend in smart mine construction. Traditional open-pit mine transportation systems rely on human power for command, which often causes vehicle delay and congestion. The operation of unmanned vehicles in an open pit mine relies on many sensors. Using big data from the sensors, we optimize vehicle paths and build an efficient intelligent transportation system. Based on large amounts of data, such as unmanned vehicle GPS data, vehicle equipment information, production plan data, etc., with the goal of reducing vehicle transportation costs, total unmanned vehicle delay time, and ore content fluctuation rate, a multi-objective intelligent scheduling model for open-pit mine unmanned vehicles was established, and it is aligned with actual open pit mine production. Next, we use artificial intelligence algorithms to solve the scheduling problem. To improve the convergence, distribution and diversity of the classical fast non-dominated sorting genetic algorithm (NSGA-II) to solve constrained high-dimensional multi-objective problems, we propose a decomposition-based constrained dominance principle genetic algorithm (DBCDP-NSGA-II), retaining feasible and non-feasible solutions in sparse areas, and compare it with four other commonly-used multi-objective optimization algorithms. Simulation analysis shows our algorithm provides the best overall performance results of the multi-objective models. Furthermore, we apply intelligent scheduling models and optimization algorithms to mining practice and obtain new truck operation routes and schedules, reducing truck operation costs by 18.2%, truck waiting time by 55.5%, and ore content fluctuation by 40.3%. For open-pit mine unmanned transportation, the approach provides a variety of optimized solutions for minimum transportation costs, minimum waiting time, minimum ore content fluctuation rate, and a balance of the three indicators. Through an artificial intelligence algorithm, this study realizes intelligent unmanned vehicle path planning and improves the operation efficiency of open-pit mine intelligent transportation systems.

INDEX TERMS Intelligent transportation system, traffic big data, unmanned driving, intelligent scheduling, NSGA-II, open-pit mine.

The associate editor coordinating the review of this manuscript and approving it for publication was J. D. Zhao .

I. INTRODUCTION

Open pit mines are constrained by factors such as multiple pieces of working face equipment, harsh environments, and

complicated working conditions. Unmanned production is an obstacle to achieve smart, unmanned mines, and current research on open pit unmanned mining is still in its infancy. Vehicles often wait in line (Figure 1), which greatly reduces production efficiency [1]. To improve the operation efficiency of vehicles, it is necessary to comprehensively consider various factors such as vehicles, crushing stations, ore grades (ore content), *etc.* to plan the vehicles' operation routes (Figure 2). Mining giant Rio Tinto Group is a global leader in automated mining and unmanned driving [2]. In 2018, Rio Tinto Group operated the world's first batch of unmanned vehicles on 1,700 kilometers of track, which increased the speed of unmanned vehicles transporting iron ore by 6% and reduced the impact of changing drivers [3]. Japanese machinery manufacturer Komatsu is introducing a global positioning system (GPS) control, is loading a large unmanned mining dump truck with a mass of 100 tons, and has conducted a trial operation on Kalimantan Island [4]. Canadian International Nickel has developed an underground communication system for trial use at the Stobie mine. The mine's scrapers, rock drilling rigs, and underground cars have all been unmanned, and workers remotely control these devices on the ground. There is basically no need to set up staff underground [5]. Australian Micromine has developed a web-based online remote mining applications control system called PITRAM to reduce mining costs by 10% [6]. With the



FIGURE 1. Vehicles waiting for unloading.

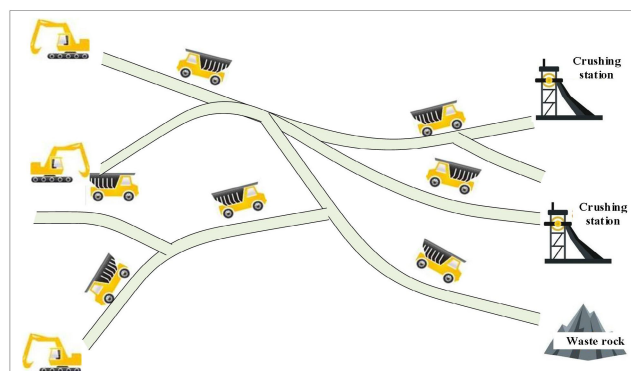


FIGURE 2. An abstract basic model of open-pit mine vehicle scheduling.

rapid development of 5G, edge computing, big data, artificial intelligence and other technologies, open-pit mine unmanned driving technology has achieved breakthrough development. Cloud computing's centralized processing and long-distance transmission will cause network congestion [7], and the data cannot be received quickly enough to meet the real-time needs of users [8], especially in delay-sensitive use scenarios. Multiple sensors carried by unmanned vehicles continuously collect information about the external environment and generate a large amount of data. Unmanned vehicles can generate GB-level data every few seconds, which poses challenges to the calculation and storage capabilities of the vehicle itself. Unmanned driving in open pit mines has high requirements for real-time data response [9]. Compared with 4G and Wi-Fi, the 5G network can provide a more stable signal connection for unmanned vehicles in open pit mines [10]. We can use 5G's high-speed, low-latency, and high-reliability features to deploy guidance and positioning, route planning, task scheduling, motion control, information fusion and other edge applications [11]. These applications have high performance requirements for running equipment and cannot be directly calculated on mobile devices which have limited resources [12]. It is an effective method to migrate certain computationally-complex multi-objective optimization algorithms to resource-rich edges or remote clouds through computational migration technology [7]. The powerful computing power of edge computing can help realize intelligent production and operation management for an open-pit mine unmanned truck dispatching system [13]. As shown in Figure 3, the open-pit mine unmanned scheduling system consists of a set of network computing nodes (such as servers, base stations, vehicle-mounted terminals, mobile terminals, user computers, various monitoring terminals, *etc.*). In edge computing scenarios, the communication bandwidth between different nodes is very limited and heterogeneous, and different computing nodes support a wide range of computing capabilities [14]. Edge computing connects computing devices to the network, and the nodes communicate directly or indirectly, greatly reducing remote data transmission time. In a decentralized network, data can be processed not only locally, but also at other geographically-dispersed nodes [15]. Network computing nodes can perform functions such as computing offload, data caching and processing, and mobility management [16]. The integrated application of 5G, edge computing for big data computing, and artificial intelligence algorithms makes open-pit mine driverless vehicles truly achieve independent driving and autonomous path planning.

Nonlinear equation systems (NESs) are involved in many fields such as power systems, machinery manufacturing, neural networks, pattern recognition, production scheduling, network communications, investment portfolios, image processing, *etc.* Therefore, the solution of NESs has become a very important research topic. The vehicle scheduling problem (multi-objective optimization problem) in this paper is essentially a NESs problem. At present, there are many algorithms for solving NESs, which can be simply divided into

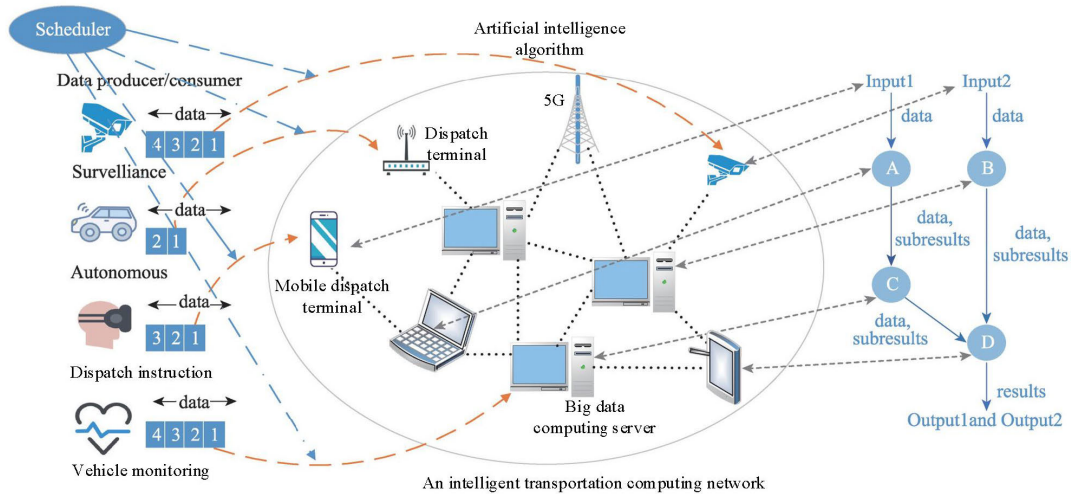


FIGURE 3. An open-pit mine vehicle scheduling system based on 5G and big data.

two types: traditional optimization algorithms and intelligent optimization algorithms. Among them, traditional optimization algorithms for solving NESs are usually iterative methods based on gradient information, such as: conjugate gradient method, Newton method, pseudo Newton's method, steepest descent method, etc.. These methods depend on the selection of the initial point. If the initial point is not selected properly, the root may not be found. Due to the need for gradient information, it is only applicable to differentiable functions, and it is easy to fall into the local optimal solution. More importantly, these methods can only find one root in a single run. The intelligent optimization algorithm is a group-based optimization algorithm, which searches from multiple points simultaneously instead of a single point search, and has invisible parallelism. And the requirements for the initial point are not high, and it is still applicable to NESs that are not differentiable. The solution range is wide, with high efficiency and robustness. It greatly facilitates the solution of NESs and solves the limitations of traditional optimization algorithms. Therefore, the use of intelligent optimization algorithms to solve NESs has attracted more and more attention, and has become a research hotspot for scholars at home and abroad in recent years. Gao *et al.* [17] designed a two-phase evolutionary algorithm TPEA (two-phase evolutionary algorithm) to solve NESs. In this algorithm, NESs are converted into single-objective optimization problems. In the first phase, niched based on crowding differential evolution (NCDE) is used, and construct the diversity index based on Gaussian kernel function to maintain the diversity of the population to achieve the balance of convergence and diversity. In specific iterations, NCDE and NSGA-II alternately produce high-quality candidate solutions. In the second stage, a detection method is designed to locate promising areas (that is, areas where the optimal solution may exist), and finally find the root of NESs through DE (differential evolution) as a local search algorithm. Gong *et al.* [18] further improved

on the basis of MONES (multi-objective optimization for nonlinear equation systems) and proposed a weight-based bi-objective optimization algorithm (A-Web). In this algorithm, the weight value in the objective function is randomly generated from 0 to 1. In the optimization process, two search algorithms, SHADE (success-history based parameter adaptation for differential evolution) and NSGA-II, are combined to produce offspring through mutation. In this process, the parameters are adaptively adjusted, which improves the accuracy of the search. The choice between individuals is then determined by the non-dominated ranking. Ojha [19] proposed the HCMOIWO (hybrid cooperative multiobjective optimization IWO) algorithm. In this algorithm, the population is divided into two subpopulations of equal size, each subpopulation corresponds to an objective function, based on IWO and STS (space transformation search) for each Search for each sub-population, and then combine all the subpopulations, and then select the next generation of individuals with non-dominant sorting, store the non-inferior individuals in each iteration generated in the predetermined archive, and finally output the individuals in the archive.

Regarding the optimization of open-pit mine excavation and transportation equipment scheduling and other operational theories, some studies have concentrated on the randomness among them, using simulation and queuing theory to model and analyze the problem. Gu Q. *et al.* [20] proposed a computational simulation model to verify the optimization effect of a mathematical programming model on the open pit mining rate, and concluded that adding vehicles does not necessarily optimize mining operations. Liu G. *et al.* [21] used the queuing theory model to evaluate the loss of mining capacity caused by production vehicle delays, thereby improving the truck scheduling constraint model for large open pit mines. Mendes *et al.* [3] proposed a new real-time three-dimensional realization method to determine the relative position of power shovels and trucks to reduce accidents

between them. The system can optimize truck dispatching. Although these studies have not directly solved the problem of open-pit mine truck dispatching, they have made great contributions to dispatching theory research and the development of truck dispatching. Wang *et al.* [22] introduced mixed ore into the scheduling model to reduce grade fluctuations during the operation of mine materials and to meet production plan and ore composition requirements. Patterson *et al.* [23] proposed a decision method based on a time-dependent Markov decision process (TiMDP) to address possible delays and overtime pay caused by queuing. Dong *et al.* [24] established a scheduling model based on predicting truck queuing time to select vehicles. Wan *et al.* [25] proposed an optimization model that minimizes the fuel consumption of dump vehicles and scrapers in open pits to meet the loading and unloading requirements of dump sites. These studies face the scheduling problem from a single perspective and establish models to reduce queue time and grade fluctuations. In the study of open-pit mine truck dispatching, computer-controlled mine truck dispatching optimization was initially adopted, and then linear planning, dynamic programming saving methods, and other scanning methods were used to finalize vehicle dispatch. Zhou *et al.* [26] developed an optimal scheduling program for open-pit mines, using a stochastically-optimized genetic algorithm to minimize vehicle wait time in the target fleet and increase production capacity. Godoy [27] developed a combined optimization algorithm based on the simulated annealing algorithm to solve the truck scheduling decision problem; Souza *et al.* [28] proposed a hybrid heuristic algorithm, which combined the greedy random adaptive search procedure and the general variable neighborhood search to optimize the minimum dispatch problem in truck scheduling. Gui J. *et al.* [29] jointly studied the application of integer programming-based methods to vehicle scheduling systems.

Some experts have studied a dynamic programming-based enumeration algorithm and applied it to optimize underground vehicle scheduling system management [30]. To solve the nonlinear scheduling problem, some experts have proposed a linear time approximation scheme for the vehicle scheduling problem [31]. Although the research on mine truck dispatching is relatively mature, most of these studies use a single target to allocate mine vehicles. However, mine truck dispatching is a complex engineering system. Considering only a single target makes it difficult to dynamically allocate and optimize the vehicles. For this problem, using multi-objective optimization, Coelho *et al.* [32] proposed three multi-objective heuristic algorithms: 2PPLS-VNS, MOVNS, and NSGA-II, which can be applied to the open-pit mining dynamic truck allocation problem. Lin B. *et al.* [33] proposed a multi-objective evolutionary algorithm, which can be applied to open-pit mine truck dynamic scheduling, and verified that in most cases it provides a good solution for all scheduling situations.

At present, most research on open-pit mine vehicle scheduling is based on the single-target model, while theoretical research on multi-objective intelligent dispatch

models is rarer. Most current multi-objective vehicle scheduling approaches target two objective functions with the smallest deviations: revenue, transportation costs, or vehicle use, and rarely consider grade fluctuation objectives. The grade is used as a constraint condition, but the grade limit can easily cause the number of optimal solutions to be few or zero. Therefore, the current vehicle multi-target scheduling model has not effectively solved many practical vehicle scheduling problems. In view of the above problems, to rationally deploy open-pit mine unmanned vehicle transportation equipment, achieving cost reduction and increased efficiency in open-pit mine enterprises, and to solve the needs of multi-objective vehicle transportation scheduling management, this article focuses on vehicle transportation costs, minimum total queuing time and the minimum grade fluctuations as objective functions. A multi-objective intelligent scheduling model for open-pit mine driverless vehicles is constructed, and then the model is solved using the modified calculation method, a decomposition constraint-dominated NSGA-II, to realize the intelligent dispatch of new open-pit mine driverless vehicles. The simulation results show that our proposed multi-objective scheduling model and intelligent solving algorithm can help reduce transportation costs, waiting time and ore grade fluctuations.

The remainder of the paper is organized as follows. In Section II, we introduce the objective functions and constraints of the multi-objective scheduling model for open-pit mine vehicles. Section III introduces an improved method for solving the multi-objective scheduling model and compares it with other classical methods. In Section IV, we apply the proposed scheduling model and optimization algorithm to mine practice. Finally, we conclude our work and discuss further work in Section V.

II. SYSTEM MODEL AND DEFINITIONS

The multi-objective scheduling optimization model for open pit mine unmanned vehicles is essentially the establishment and solution of equations. The system of equations is composed of constraints and objective functions, and then an intelligent algorithm is used to solve the system of equations to obtain the vehicles' running route and scheduling time, as shown in Figure 4.

A. MULTI-OBJECTIVE OPTIMIZATION MODEL OBJECTIVE FUNCTION CONSTRUCTION

The optimization goals involved in unmanned vehicle dispatching in open pit mines are: minimum total transportation volume, maximum output, minimum vehicle waiting time, *etc.* The objective functions of commonly-used scheduling models are mainly the smallest total transport volume and the largest output. In practice, mining companies are more concerned about how to reduce transportation costs (*i.e.*, total transportation volume), as well as increase production and equipment utilization. The largest output and the highest equipment utilization rate are a mine's ultimate goals. One quantitative feedback parameter associated with

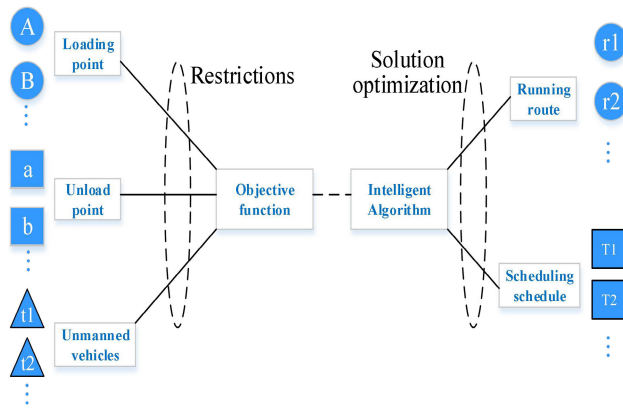


FIGURE 4. The general multi-objective scheduling optimization model.

this goal is truck waiting time, which reflects the equipment utilization rate and output. The vehicle capacity and the output is increased when waiting time is lower. For metal open-pit mines, grade is also a scheduling requirement. In previous studies, from real-time mine feedback, the grade should not be below the prescribed limit, otherwise it will have a large impact on its subsequent beneficiation. To maximize resource use and promote sustainable production, the deviation of the actual grade from the set value is minimized; the deviation of grade is often used as the criteria. Another reason for considering grade deviation is that in the gradual mining process, when scheduling problems make it difficult to meet grade limits, a reasonable and feasible scheduling scheme can be found through grade deviation.

This study comprehensively considers many mine truck scheduling factors. Based on the concerns of mining companies, a general multi-objective optimization model for truck scheduling is built with the goals of minimum total truck waiting time, minimum transportation cost and minimum grade deviation. Each model optimization goal is represented by a function, and all scheduling parameters are collectively called S. The constructed multi-objective optimization goal function is shown in Formula 1. The objective function $F_1(s)$ is the minimum transportation cost, $F_2(s)$ is the minimum total truck waiting time, and $F_3(s)$ is the minimum ore grade deviation. The meaning of the symbols in the formula is shown in Table 1.

$$F(S) = \text{Minimizar} [F_1(S), F_2(S), F_3(S)] \quad (1)$$

$$F_1(S) = \min \sum_{r=1}^k \left(\sum_{i=1}^n \sum_{j=1}^m d_{ij} C_{r1} x_{rij} + \sum_{i=1}^n \sum_{j=1}^m d_{rij} C_{r2} y_{rij} + \sum_{r=1}^k \Delta T_r C_{r3} \right) \quad (2)$$

TABLE 1. Symbol meaning.

Symbol	Description
i	The i -th loading point
j	The j -th unloading point
d_{ij}	Distance from loading point i to unloading point j
c_r	r truck capacity
c_{r1}	Reload cost of vehicle r
c_{r2}	No-load cost of vehicle r
c_{r3}	Car repair cost
x_{rij}	The number of times the r -th truck goes from the i -th loading point to the j -th unloading point
y_{rij}	The number of times the r -th truck goes from the j -th unloading point to the i -th loading point
ΔT_r	Running time of vehicle r
T_{limit}	Shift working time or single optimization time
T_{zrij}	Heavy truck running time from the i -th loading unloading point of the r -th vehicle
T_{qrij}	Empty truck running time from j -th unloading point to i -th loading point
T_{x_r}	Idle time of r vehicle
g_i	Grade of loading point i
G_a	Target ore grade

$$F_2(S) = \min \sum_{r=1}^k \left(T_{limit} - \sum_{i=1}^n \sum_{j=1}^m T_{zrij} x_{rij} - \sum_{i=1}^n \sum_{j=1}^m T_{qrij} y_{ij} - T_{x_r} \right) \quad (3)$$

$$F_3(S) = \min \frac{\sum_{j=1}^n \left| \sum_{r=1}^k \sum_{i=1}^m (g_i - G_a) \cdot c_r x_{rij} \right|}{\sum_{r=1}^k \sum_{j=1}^n \sum_{i=1}^m c_r x_{rij}} \quad (4)$$

B. MULTI-OBJECTIVE OPTIMIZATION MODEL DATA SOURCES AND PROCESSING CONSTRAINTS

The constraints of a multi-objective optimization model are basically the same as those of a single-objective optimization model. The grade constraints of a multi-objective optimization model can be ignored when it is difficult to meet the ore grade requirements, and a reasonable and feasible plan can be obtained with a grade deviation target. The specific constraints of the truck scheduling multi-objective optimization model are as follows:

The output should meet the requirements of each unloading point:

$$\theta_1(x) = \sum_{r=1}^k \sum_{i=1}^n c_r x_{rij} - f_j \geq 0 \quad (5)$$

In Formula 5: f_j is the output requirement of the unloading point.

The total amount transported out of the i -th loading point cannot be greater than the total capacity of the i -th loading point:

$$\theta_2(x) = \sum_{r=1}^k \sum_{j=1}^n c_r x_{rij} - g_i \leq 0 \quad (6)$$

In Formula 6: g_i is the total amount from all loading points.

The number of loading times at the loading point is less than the maximum number of loading points within a shift:

$$\theta_3(x) = \sum_{r=1}^k \sum_{j=1}^m x_{rj} - B_c \leq 0 \quad (7)$$

In Formula 7: B_c is the maximum number of loading points in a shift.

The total unloading of the j -th unloading point cannot be greater than the maximum unloading value of the unloading point:

$$\theta_4(x) = \sum_{r=1}^k \sum_{i=1}^m c_r x_{ij} - q_j \leq 0 \quad (8)$$

In formula 8: q_j is the maximum value of the unloading point.

The grade of unloaded ore needs to meet the restriction requirements:

$$\theta_5(x) = \left| \frac{\sum_{r=1}^k \sum_{i=1}^n c_r x_{ij} \times a_i}{\sum_{r=1}^k \sum_{i=1}^n c_r x_{ij}} - e \right| - \alpha\% < 0 \quad (9)$$

In formula 9: e is the grade limit; $\alpha\%$ is the grade tolerance; a_i is the grade at loading point i .

The number of transportation times on each route:

The n loading points are divided into p ore loading points and $n-p$ rock loading points, and the m unloading points are divided into q ore unloading points and $m-q$ rock unloading points. In the mining process, ore and rock are produced. Formula 10 shows that the vehicles loaded with ore cannot go to the point where the rock is unloaded.

$$\begin{aligned} &\text{while } i = p, j = q \text{ or } i = n - p, j = m - q, \\ &x_{rij} \in \{0, 1, 2, 3 \dots\}, y_{rij} \in \{0, 1, 2, 3 \dots\}; \\ &\text{otherwise } x_{rij} = 0, y_{rij} \in \{0, 1, 2, 3 \dots\}. \end{aligned} \quad (10)$$

III. OUR PROPOSED DBCDP-NSGA-II ALGORITHM

A. DBCDP-NSGA-II ALGORITHM

The fast, non-dominated sorting genetic algorithm (NSGA-II) adds an elite retention strategy based on NSGA. First, randomly generate N individuals as parents P_t , and obtain N children Q_t through cross mutation; the children and the parent are merged from $R_t = P_t \cup Q_t$. Select N individuals with high priority from R_t to enter the next generation. Before selection, sort R_t non-dominantly, let the number of dominating individuals be X_a , dominate the set S_a , and if $a > b$, then dominate a set $S_a = S_a \cup \{b\}$, and dominate the number of b individuals $X_b = X_b + 1$. Put the individuals with $X = 0$ into F_1 ; F_2 is the non-dominated individual in the evolutionary population excluding F_1 's dominant individual, F_3 is the non-dominated individual in the evolutionary population excluding F_2 's dominant individual, etc. Divide each solution into levels, $I = \{F_1 \cup F_2 \cup \dots \cup F_{l-1}\}$, $T = \{F_1 \cup F_2 \cup \dots \cup\}$, when the number of sets I is less than N , and the number

of T is greater than N , it is called the critical layer, and the critical layer is reordered using crowding degree to select the N best individuals for the next generation [34]. When NSGA-II is dominating the ranking, the optimal solution only depends on the fitness function. As the target dimension increases, this dominance relationship will cause the selection pressure to decrease significantly when approaching the optimal frontier, so that a large number of equivalent solutions exist [35]. To this end, this paper proposes that after the child and the parent are merged, any duplicate solution is eliminated, and then crossover and mutation are performed until $2N$ different solutions are generated, and then sorted. In the sorting, decomposition and constraint domination are used to penalize the equivalent solutions that Pareto dominates, thereby increasing the selection pressure of the algorithm.

This study combines three methods, Pareto domination, decomposition-based and constraint domination, to form a new domination method, DBCDP domination. This domination approach first uses the Pareto dominance solution for quick sorting, and then the decomposition and constraint domination are equivalent to the penalty. DBCDP domination mainly uses Pareto dominance, the constraint violation degree, and solution density to select the best individuals to improve the protection of non-feasible solutions in sparse areas that are close to feasible areas.

Due to the different nature of the u and v solutions, the decomposition constraint domination can be divided into three cases:

When both u and v are feasible and equivalent solutions, if u and v match the same weight vector, then the convergence of the solution is judged according to the value of d_1 , and the closest point to the ideal point is selected as the solution; if u and v correspond to different weight vectors, then the solution density is determined based on the value of RP_j , and the solution closest to the ideal point and that with the smallest density are selected.

When both u and v are infeasible solutions and are not dominated by Pareto, if u and v are attached to the same weight vector, then the distance between the solution and the feasible region is determined according to the degree of constraint violation, and the closest feasible option is selected. Otherwise, select the sparse area solution as the domain solution according to the degree of constraint violation and the value of RP_j .

When u is a feasible solution and v is an infeasible solution, the density of the solution is judged according to the value of RP_j , and the sparse area solution is selected, thereby improving the ability of the population to explore the unknown field.

According to the analysis of the above three situations, the decomposition constraint dominance relationship is defined as follows: given a set of weight vectors R , u and v are two solutions in the population P . If one of the following statements holds, the solution u DBCDP dominates the solution v .

1) u AND v ARE BOTH FEASIBLE SOLUTIONS

u Pareto dominates v ; u and v are Pareto equivalent solutions, $RP(u) = RP(v)$, $d_1(u) < d_1(v)$; or $RP(u) \neq RP(v)$, $d_1(u) < d_1(v)$ $RP_j(u) < RP_j(v)$.

As shown in Figure 5, u , v , and y are feasible solutions and the two Paretos are equivalent, because $RP(y) = RP(v)$ and $d_1(y) < d_1(v)$; that is, y DBCDP dominates v . Because $RP(u) \neq RP(v)$, $d_1(u) < d_1(v)$ and that is u DBCDP dominates v .

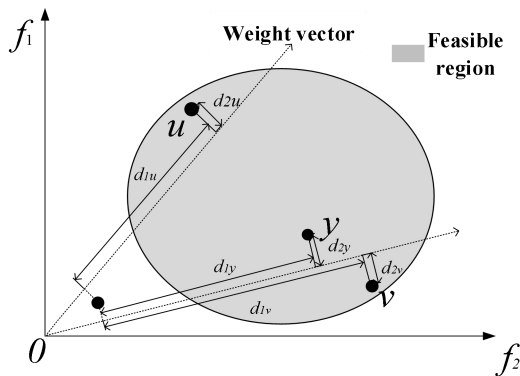


FIGURE 5. u , v , y is the feasible solution distribution.

2) BOTH u AND v ARE INFEASIBLE SOLUTIONS

u Pareto dominates v ; u and v are Pareto equivalent solutions. $RP(u) = RP(v)$, $VFD(u) < VFD(v)$ or $RP(u) \neq RP(v)$, $VFD(u) < VFD(v)$, $RP_j(u) < RP_j(v)$.

As shown in Figure 6, u , v , and y are non-feasible solutions but the two Paretos are equivalent, because $RP(y) = RP(v)$, $VFD(y) < VFD(v)$; that is, y DBCDP dominates v . $RP(u) \neq RP(v)$, $VFD(u) < VFD(v)$, $RP_j(u) = 1 < RP_j(v) = 2$; that is, u DBCDP dominates v .

3) ONLY ONE OF u AND v IS A FEASIBLE SOLUTION

u is a feasible solution, v is a non-feasible solution and $RP_j(u) < RP_j(v)$. To clearly illustrate the role of DBCDP domination, Figure 7 shows the use of Pareto dominance and DBCDP dominance, pairing DTLZ8 test questions to 19 randomly generated solutions for non-dominated sort results. For each solution, mark the DBCDP dominance order on the right and the Pareto dominance rank on the left (number of layers).

Figure 6 shows that the four Pareto equivalent solutions (A, B, C, and D) that constitute the first layer of non-dominated frontiers are subdivided into two DBCDP dominated frontiers when using DBCDP dominated sorting. The first category is $C1 = \{A, B, D\}$, which contains two extreme individuals A and D and the solution B with the smallest d_1 distance and associated with the least-crowded weight vector. The second category is $C2 = \{C\}$, which has a larger distance d_1 and a higher density of its associated weight vectors. According to d_1 and RP_j , DBCDP penalizes the rank of certain Pareto solutions. The figure also shows that DBCDP

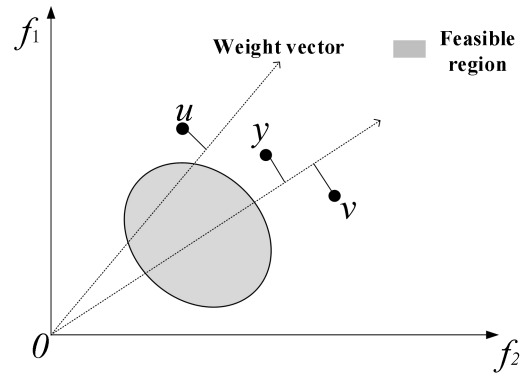


FIGURE 6. u , v , y is the infeasible solution distribution.

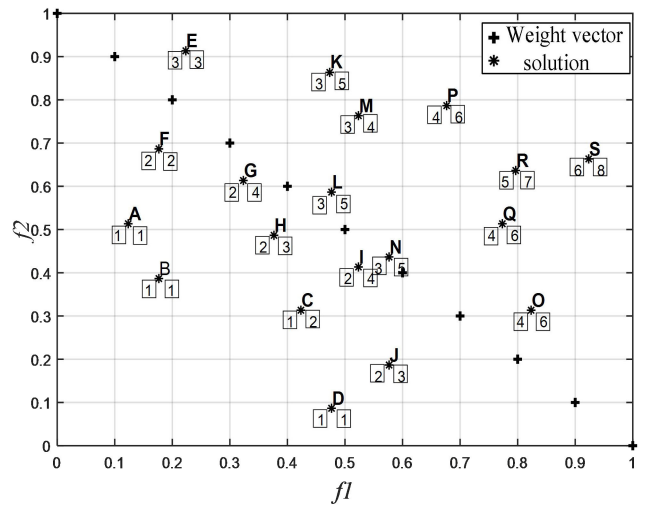


FIGURE 7. Pareto dominance and DBCDP dominance of the 19 randomly-generated solutions of DTLZ8 for sorting.

supports 8 layers of solutions. The Pareto domination has a 6-layer solution. It shows that the selection pressure of the DBCDP domination is stronger than the traditional Pareto domination. It is further proven that the DBCDP domination can punish the Pareto equivalent solution.

B. PARAMETER SETTING AND ALGORITHM COMPARISON

Experimental environment: Inter Core (TM) i5-2450M CPU, 4 GB memory, Windows 10 operating system, Matlab version R2017a. Parameter setting: the number of decision variables = $10 * M$, the number of objective functions $M = 5, 8, 12, 16, 20$, the population size is 100. Study [36] uses a weight vector to protect the algorithm diversity, so the number of weight vectors is the same as the size of the population. Select the analog binary for the crossover method, crossover rate = 0.5, mutation rate = 0.02. Mutation step size = $0.1 * (\text{upper limit of decision variables} - \text{lower limit of decision variables})$; the maximum number of iterations is 100. This experiment studies the performance of DBCDP-NSGA-II on the constrained DTLZ [37]–[39] test problem. The DTLZ test function is one of the

Algorithm 1 DBCDP-NSGA-II Algorithm

1. Randomly generate N individuals in the decision space to form the initial population P_t and calculate its objective function value and constraint violation.
2. Cross-mutate the population P_t to form progeny Q_t until $2N$ different individuals are produced.
3. Normalize R_t , calculate the ideal point Z^* of R_t , and find the weight vector for each solution in R_t .
4. Determine the rank of each individual according to the DBCDP domination method; strictly rank according to the sought rank.
5. Store F_1, F_2, \dots, F_{l-1} in order, and then sort the critical layer for crowding degree until N optimal individuals are selected to form a new population P_{t+1} .
6. Clear the rank of the population.
7. When $t + 1$ is greater than the maximum number of iterations, the operation is ended; otherwise, return to step 2.

most extensive test functions for evaluating the performance of a high-dimensional, multi-objective evolutionary algorithm [40]–[42]. The constrained DTLZ test functions selected in this experiment are mainly divided into two categories, the first category are C-DTLZ1 and C-DTLZ2 with only one constraint; the second category are DTLZ8 and DTLZ9 with M constraints.

The optimal frontier value of the C-DTLZ1 test function is the same as the DTLZ1 hyperplane, and there is an infeasible area obstacle caused by a constraint when approaching the optimal frontier, which makes the algorithm more difficult to converge.

In the C-DTLZ2 problem, a constraint is introduced to make the optimal frontier of DTLZ2 into an unconnected optimal frontier. Only the target space located in the $(M+1)$ hypersphere with radius r is the feasible domain. The function tests whether the algorithm has the ability to handle disconnected frontiers.

The Pareto optimal solution for the DTLZ8 test function consists of a straight line and a hyperplane, where the straight line is determined by the first $(M-1)$ constraints and the hyperplane is determined by the M th constraint.

The Pareto optimal solution of the DTLZ9 test function is the intersection of the first $(M-1)$ objective function constraints. In the two-dimensional Pareto optimal solution graph, the optimal solution is the quarter circle of the unit circle arc. Most optimization algorithms have difficulty finding the global optimal solution of DTLZ9 and can only find the optimal solution in a certain area.

The algorithm comparison approach is as follows: to verify the DBCDP-NSGA-II algorithm proposed in this study, four constrained multi-objective optimization algorithms: NSGA-II(C-NSGA-II), C-NSGA-III, C-MOEA/D, and C-MOEA/DD are selected and compared. We introduce

the Deb constraint criterion for comparative experimental research.

C. SIMULATION RESULTS

In order to compare the performance of different algorithms, the inverse generation distance (IGD) is selected as the performance index of the evaluation algorithm. IGD measures the average distance of all approximate solutions generated by MOEA (multiobjective evolutionary algorithm) to the true Pareto optimal sets. The lower the value of IGD, the closer the solution sets to Pareto optimal sets. This indicator comprehensively evaluates the convergence and distribution of the algorithm.

This article presents the results of the DBCDP-NSGA-II algorithm on the C-DTLZ1, C-DTLZ2, DTLZ8 and DTLZ9 test questions, and compares it with C-NSGA-II, C-MOEA/D, C-MOEA/DD, and C-NSGA-III. In the results comparison, the Wilcoxon rank sum test [43], [44] is used to compare the differences between the detection algorithms. For a 95% confidence, the symbols “-”, “+” and “=” indicate the statistical test results. “+” indicates a significant advantage, “-” indicates a significant inferiority, and “=” indicates no difference from DBCDP-NSGA-II.

It can be seen from Table 2 that in the C-DTLZ1 and C-DTLZ2 test functions with only one constraint, the IGD results of DBCDP-NSGA-II are relatively small, and the optimal solutions are significantly better than C-NSGA-II, C-NSGA-III, C-MOEA/D, and C-MOEA/DD. The C-NSGA-II and C-MOEA/D in the C-DTLZ1, C-DTLZ2 test problem obtained large IGD value, indicating that these two algorithms did not accurately find the location of the feasible region. The main reason is that as the number of targets increases, the ability of one solution to dominate the other decreases, and these two algorithms place too much emphasis on feasible solutions over non-feasible solutions, making the algorithm prone to local optimal solutions. In the case of C-DTLZ1, when $M=5$, C-NSGA-III is significantly better than DBCDP-NSGA-II. For the concave function C-DTLZ2, when $M=12, 16$, C-MOEA/DD obtains the optimal value second only to DBCDP-NSGA-II. The main reason is that the C-NSGA-III algorithm too discards the non-feasible solution in the sparse area and close to the feasible region. Although C-MOEA/DD retains the non-feasible solution of the sparse area in the championship selection stage, it emphasizes that the feasible solution dominates the non-feasible solution in the domination stage. DBCDP-NSGA-II emphasizes the non-feasible solution to retain sparse areas in the championship selection and domination phases. Therefore, better results can be achieved.

Table 3 shows that for the second type of DTLZ8 and DTLZ9 test problems with M constraints, DBCDP-NSGA-II finds that the result of IGD is relatively small, and the optimal solution is significantly better than C-NSGA-II, C-NSGA-III, C-MOEA/D, and C-MOEA/DD. C-NSGA-II and C-MOEA/D still have not obtained a better optimal solution. The optimal solution consists of a straight line

TABLE 2. IGD mean and standard deviation of C-DTLZ1 and C-DTLZ2 test functions.

Test function	Number of decision variables	Number of goals	C-NSGA-II		C-NSGA-III		C-MOEA/D		C-MOEA/DD		DBCDP-NSGA-II	
			Average value (AV)	Standard deviation (SD)	AV	SD	AV	SD	AV	SD	AV	SD
C-DTLZ1	50	5	5.6182e-1	6.12e-1	5.0589e-2+	8.95e-1	5.6930	3.21e-1	5.156	7.58e-1	5.173	5.08e-1
C-DTLZ1	80	8	2.7278e-1	3.87e-1	1.9901e-1	4.54e-1	2.8935	6.75e-1	1.564	6.62e-1	1.1517e-1	6.92e-1
C-DTLZ1	120	12	1.9925e-1	3.39e-1	1.6007e-1	7.08e-1	1.8022	4.01e-1	1.537	5.33e-1	1.3589e-1	5.41e-1
C-DTLZ1	160	16	3.1532e-1	5.33e-2	2.3754e-1	4.46e-1	2.4913	3.74e-1	2.324	8.48e-2	2.2321e-1	4.30e-2
C-DTLZ1	200	20	3.9577e-1	7.70e-2	2.8180e-1	7.09e-1	3.2530	4.32e-1	2.438	7.71e-1	2.3935e-1	7.87e-1
C-DTLZ2	50	5	4.0071e-1	1.33e-1	1.9126e-1	8.05e-1	2.5690	2.11e-1	1.899	5.24e-1	1.3266e-1	5.99e-2
C-DTLZ2	80	8	3.5925e-1	3.39e-1	2.4007e-1	7.08e-1	3.8022	2.01e-1	2.537	7.33e-1	2.2867e-1	5.11e-2
C-DTLZ2	120	12	3.7278e-1	3.87e-1	2.6935e-1	6.75e-1	2.9901	4.54e-1	2.564	6.62e-1	2.4200e-1	3.74e-2
C-DTLZ2	160	16	3.6182e-1	6.12e-1	2.9519e-1	8.95e-1	3.6930	9.21e-1	2.136	6.58e-1	2.1089e-1	6.21e-2
C-DTLZ2	200	20	5.4657e-1	6.98e-2	3.8945e-1	6.96e-1	5.0446	4.75e-1	3.690	7.10e-2	3.3983e-1	6.62e-2

TABLE 3. IGD mean and standard deviation of DTLZ8 and DTLZ9 test functions.

Test function	Number of decision variables	Number of goals	C-NSGA-II		C-NSGA-III		C-MOEA/D		C-MOEA/DD		DBCDP-NSGA-II	
			Average value (AV)	Standard deviation (SD)	AV	SD	AV	SD	AV	SD	AV	SD
DTLZ8	50	5	4.6846e-1	4.16e-2	2.6132e-1	6.52e-2	3.6686	2.14e-2	2.529	4.18e-2	2.2796e-1	4.20e-2
DTLZ8	80	8	5.5628e-1	4.58e-2	2.4686e-1	7.79e-2	4.8036	3.56e-2	2.889	5.73e-2	2.4201e-1	5.95e-2
DTLZ8	120	12	5.7591e-1	4.57e-2	2.1929e-1	7.50e-2	5.2379	2.89e-2	2.0454e-1	5.63e-2	2.660	6.40e-2
DTLZ8	160	16	6.5459e-1	4.65e-2	3.7263e-1	5.71e-2	5.5847	5.60e-2	3.603	4.38e-2	3.5715e-1	6.05e-2
DTLZ8	200	20	7.7996e-1	4.76e-2	4.7181e-1	5.20e-2	7.0303	5.43e-2	4.324	4.71e-2	4.2876e-1	6.51e-2
DTLZ9	50	5	4.0968e-1	1.04e-1	3.6296e-1	6.50e-1	3.9746	2.73e-1	3.569	6.62e-1	3.0131e-1	6.90e-1
DTLZ9	80	8	5.5451e-1	2.01e-1	4.4987e-1	3.20e-1	5.1438	2.04e-1	4.594	5.83e-1	4.2120e-1	7.64e-1
DTLZ9	120	12	5.0525e-1	2.77e-1	3.5308e-1	5.13e-1	4.7616	7.79e-1	3.520	6.35e-1	3.4407e-1	5.31e-1
DTLZ9	160	16	5.9329e-1	4.20e-1	4.8198e-1	6.21e-1	5.4714	7.99e-1	4.881	7.59e-1	4.864	6.91e-1
DTLZ9	200	20	6.7921e-1	6.43e-1	5.5584e-1	7.84e-1	6.8689	4.55e-1	5.653	7.58e-1	5.2651e-1	7.18e-1

and a hyperplane in the DTLZ8 example; when M = 12, C-MOEA/DD achieves the optimal frontier value, and C-NSGA-III results are significantly better than DBCDP-NSGA-II. When M = 5, 16, and 20, the C-MOEA/DD result is second only to DBCDP-NSGA-II. For the DTLZ9 test function consisting of a curve at the front of Pareto, when M = 5 and 12, C-MOEA/DD is second only to DBCDP-NSGA-II. When M=16, C-NSGA-III is significantly better than DBCDP-NSGA-II. C-NSGA-III and C-MOEA/DD all evenly divide the target space by the reference point, and

the solution corresponds to the reference point one-by-one. DBCDP-NSGA-II uses a uniformly-distributed weight vector to distribute the solution to the area closest to itself. There is no one-to-one correspondence, which improves the uniform distribution of the population. Figure 8 shows the DTLZ8 test function results from C-NSGA-II, C-NSGA-III, C-MOEA/D, C-MOEA/DD, and DBCDP-NSGA-II, iterated 50 times when M=3. The results in the figure show that the distribution of C-NSGA-II solutions is poor, while the solutions of C-NSGA-III, C-MOEA/D, C-MOEA/DD, and

TABLE 4. Average of the run-time obtained by the five algorithms on DTLZ instances with different number o objectives.

Test function	Number of goals	C-NSGA-II	C-NSGA-III	C-MOEA/D	C-MOEA/DD	DBCDP-NSGA-II
C-DTLZ1	5	19.01	20.89	18.50	19.20	18.34
C-DTLZ2		21.44	20.53	20.34	21.79	19.79
DTLZ8		19.72	22.88	21.03	20.43	18.72
DTLZ9		19.54	21.52	22.50	26.84	19.03
C-DTLZ1	8	67.12	45.17	52.91	43.92	39.56
C-DTLZ2		70.33	49.47	55.33	46.32	42.18
DTLZ8		65.87	47.01	53.03	43.34	40.01
DTLZ9		69.39	49.38	53.89	41.57	41.05
C-DTLZ1	12	120.31	80.32	103.63	84.25	50.23
C-DTLZ2		132.41	85.19	111.07	89.59	54.92
DTLZ8		119.34	81.21	104.58	88.28	57.13
DTLZ9		114.38	86.02	103.26	85.02	58.07
C-DTLZ1	16	230.14	110.38	198.53	165.09	70.03
C-DTLZ2		240.38	115.01	212.24	188.13	84.18
DTLZ8		225.39	107.24	203.78	171.21	72.19
DTLZ9		229.43	119.64	202.50	189.45	74.06
C-DTLZ1	20	563.67	179.87	400.72	273.16	120.02
C-DTLZ2		575.33	189.12	412.63	290.94	129.89
DTLZ8		557.87	183.91	402.62	282.56	130.33
DTLZ9		567.35	194.83	404.96	285.87	137.96

DBCDP-NSGA-II are more evenly distributed on straight lines and hyperplanes.

Considering the randomness in the MOEA testing process, we conducted 20 sets of experiments, each of which was run 30 times. The Wilcoxon rank sum test results show that in the 20 sets of mathematical experiments, DBCDP-NSGA-II is 20 times better than C-NSGA-II, 17 times better than C-NSGA-III, 20 times better than C-MOEA/D, and 18 times better than C-MOEA/DD. In the C-DTLZ1, C-DTLZ, DTLZ8 and DTLZ9 test problems, DBCDP-NSGA-II achieved better results on IGD indicators than C-NSGA-II, C-NSGA-III, C-MOEA/D, and C-MOEA/DD.

The computational complexity of DBCDP-NSGA-II mainly stems from selection operations and infeasible solution screening. The calculation of the selection operation mainly comes from the calculation of the convergence measure and the distribution measure. The computational complexity of the population normalization is $O(MN)$, the computational complexity of the population convergence measure is $O(MN)$, and the computational complexity of its distribution measure is $O(N^2)$. In order to obtain a population of size N , you need to compare N times, the required computational complexity is $O(N)$, the computational complexity of the above four-step selection operation is $O(N^2)$. Both the distribution measure and the convergence measure in the selection of infeasible solutions can be obtained through the selection operation without repeated calculations. In order to obtain N infeasible solutions, the required computational complexity is $O(N)$. Finally, the computational complexity of DBCDP-NSGA-II is $O(N^2)$. C-NSGA-II needs to calculate the two parameters of the dominated number n_p of each individual p and the set S_p of solutions dominated by the individual. Traversing the entire population, the computational complexity of this

parameter is $O(MN^2)$. The computational complexity of C-NSGA-III is mainly composed of non-dominated sorting and population distribution maintenance strategies. The computational complexity of both parts is $O(MN^2)$, so the computational complexity of C-NSGA-III is $O(MN^2)$. The computational complexity of C-MOEA/D mainly comes from selecting the neighborhood of the reference direction, updating the reference point and updating the population. The computational complexity of the selection of the neighborhood of the reference direction is $O(MN^2)$, and the computational complexity of updating the reference point and updating the population are both $O(MN)$, so the computational complexity of C-MOEA/D is $O(MN^2)$. The computational complexity of C-MOEA/DD mainly comes from the selection of the neighborhood and niche strategy of the reference direction, and its computational complexity is $O(MN^2)$. The computational complexity of DBCDP-NSGA-II is lower than that of the other four comparison algorithms, especially when the target dimension is high, the computational complexity of our proposed algorithm is more obvious. It can be seen from Table 4 that for all the test functions on the targets of 5, 8, 12, 16, and 20, the operation runtime of DBCDP-NSGA-II proposed in this paper is the shortest. Although it is not much different from the other four comparison algorithms on the 5-dimensional targets, as the target dimension increases, the algorithm using the selection operation of this article shortens the running time more and more than other comparison algorithms, especially at the 20 targets. The C-NSGA-II with the longest running time is shortened by an average of nearly 435s, and the average running time of the four comparison algorithms is shortened by 227s. This shows that the selection operation proposed in this paper can improve the convergence speed and the higher the target dimension, the more obvious the advantage.

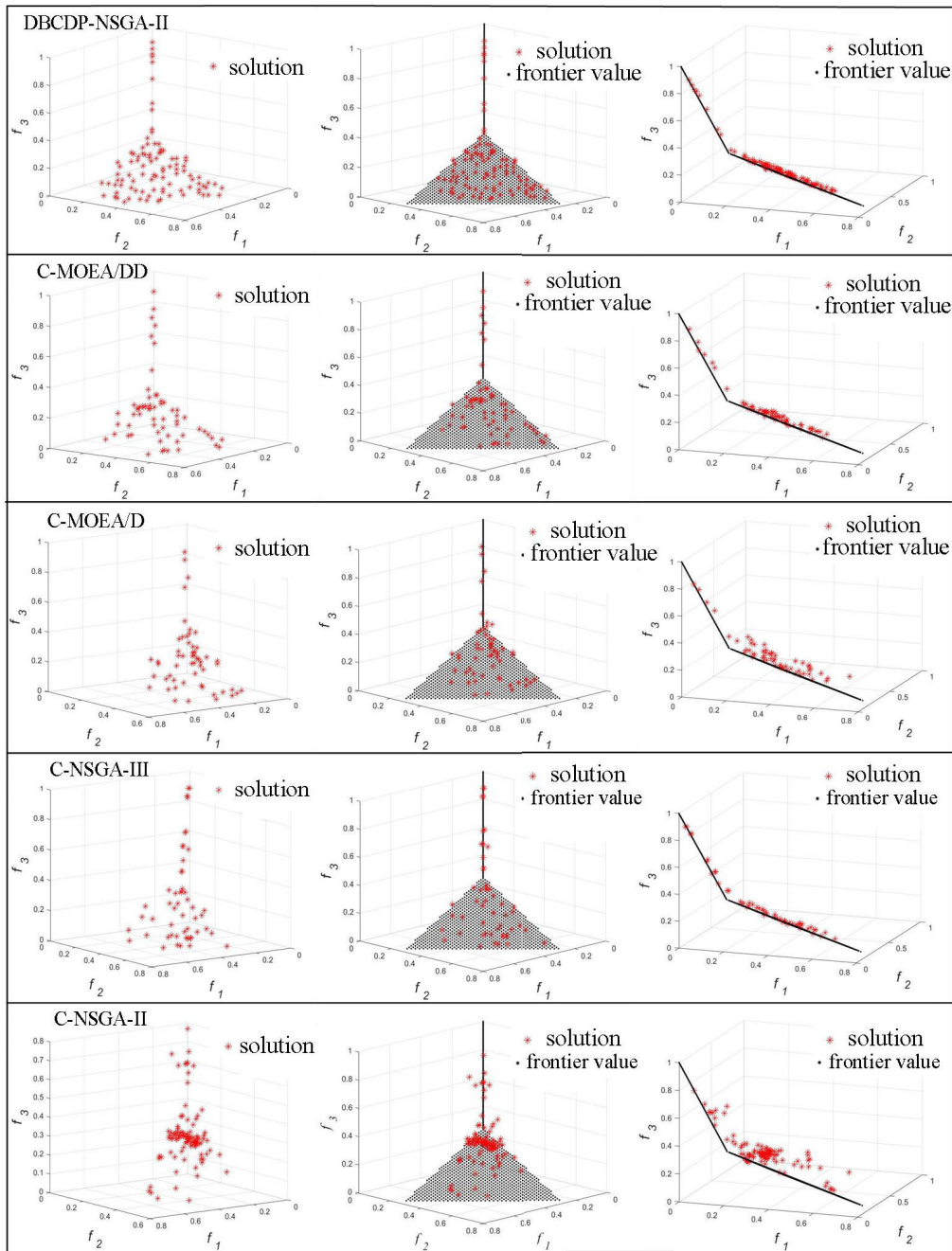


FIGURE 8. Results of C-NSGA-II, C-NSGA-III, C-MOEA/D, C-MOEA/DD, and DBCDP-NSGA-II for the DTLZ8 test function.

IV. PERFORMANCE ANALYSIS

Optimize the intelligent scheduling of unmanned vehicles in an open-pit mine intelligent mining area (Figure 9), and extract the necessary parameters, such as the cost per unit distance of a heavy truck, the average speed of a heavy truck, the weight of an unmanned vehicle, the unmanned vehicle GPS data, and the target ore grade of the unloading point information. DBCDP-NSGA-II is used to optimize the multi-objective intelligent scheduling.

A. DATA ACQUISITION

1) TRUCK DATA

There are 20 unmanned vehicles, 6 loading sites and 3 crushing stations in this open-pit mine intelligent mining area. Among them, the No. 1 and No. 2 crushing stations each have a capacity of 30 thousand tons, and the No. 3 crushing station has a capacity of 25 thousand tons. The lowest grade limit is 0.090%. The fuel consumption of unmanned vehicles is 6.38 L/km when loaded and 1.98 L/km when empty.



FIGURE 9. Intelligent mining area of an open pit mine.

Match the GPS data according to the driving trajectory of the unmanned truck, analyze the speed of the vehicle under heavy load and no load, and take the average. The unloaded speed of the unmanned truck is 20 km/h and the heavy load speed is 16 km/h. According to historical data statistics, the loading time for driverless vehicles is set at 5 minutes, and the unloading time is 3 minutes. The working capacity of the crushing station is 10,000-14,000 tons.

2) DEVICE PARAMETERS

The relevant parameters for the excavator and crusher are shown in Table 5 and Table 6.

TABLE 5. Excavator parameters.

Device name	Device model	Length, Width, Height (mm)	Bucket volume (m ³)	Working weight (kg)	Working efficiency (t/h)
Single bucket excavator	XG836	11170, 3340, 3239	1.8	33800	650

TABLE 6. Crusher parameters.

Equipment name	Device model	Feed port width (mm)	Total weight of equipment (T)	Production capacity (T/h)
Hydraulic Gyratory Crusher	PXZ1200 /160	1200	215.0	1250-1480

3) DISTANCE FROM LOADING POINT TO UNLOADING POINT

According to the running GPS data for the vehicles in the intelligent dispatch system, determine the distance between the various stations. For example, calculate the distance from loading point A to crushing station a, and find the GPS data of the vehicle running between loading point A and crushing

station a. From the data, the driving trajectory of the driverless truck and the corresponding time node can be derived, and then the travel distance calculated for the two corresponding latitudes and longitudes in the time period from the beginning to the ending point. Next, add up the distances between loading point A and crushing station a. To obtain more accurate data, select 10 vehicles, and perform 5 calculations for each vehicle to obtain the distance between loading point A and crushing station a. The distance matrix between each loading point and each unloading point is shown in Table 7.

TABLE 7. Distance from loading point to unloading point (km).

Crushing station	Loading point					
	A	B	C	D	E	F
a	2.872	3.231	1.348	2.964	2.165	2.592
b	3.075	1.981	1.865	2.134	1.753	1.962
c	2.349	1.658	2.031	0.805	1.596	1.640
d	3.689	2.769	3.421	3.465	2.769	2.524

4) ORE GRADE AND AMOUNT OF ORE AT EACH LOADING POINT

Table 8 shows the ore demand and ore grade content of each loading point.

TABLE 8. Shovel quantity (10,000 tons) and grade content of each loading point.

Loading point	A	B	C	D	E	F
Ore amount	0.61	0.49	0.72	0.53	0.65	0.58
Ore Grade	0.11%	0.15%	0.11%	0.13%	0.13%	0.12%

5) TRUCK FREIGHT

The transportation costs of driverless vehicles mainly include fuel consumption and maintenance costs. Many factors affect fuel consumption, such as speed, slope, load capacity, weather, and road conditions, among which weather and road conditions are uncontrollable. Fuel consumption is difficult to quantify, so the cost is based on historical data and work experience: the average heavy-load cost is 28 yuan/km, the average no-load cost is 22 yuan/km, and the average maintenance cost, including inspection costs, is 1 yuan/h.

B. RESULT ANALYSIS

The solution result from DBCDP-NSGA-II is shown in Figure 10. Figure 10 shows that the three objectives of the truck scheduling problem are optimized, and the DBCDP-NSGA-II is used to solve the pareto optimal frontier. The trend between some targets is more obvious. Solve the three objectives to get the pareto optimal front surface, as shown in Figure 10(a). For the optimization between the transportation cost and the total waiting time, there is a certain change rule of concave advantage, as shown in Figure 10(b). When the transportation cost decreases, the waiting time increases, which is consistent with the objective function. At the scene, the greater the waiting time, the vehicle will

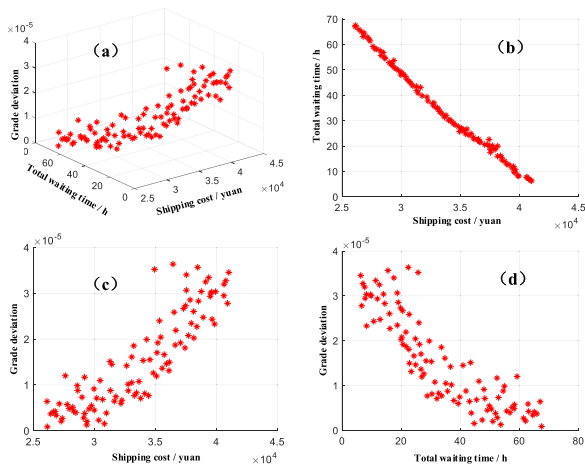


FIGURE 10. DBCDP-NSGA-II example optimization results. (a) Optimal frontier view. (b) Target optimization of transportation costs and total waiting time. (c) Target optimization of transportation costs and grade deviation. (d) Total waiting time and optimization of grade deviation target.

be sent to the same crushing station and loading point, the waiting time of the vehicle will increase, and the fewer the number of transports, the lower the vehicle transportation cost. This change does not change linearly, it is a curve change with a slightly concave shape. For the optimization between the transportation cost and the target grade deviation, as shown in Figure 10(c), when the transportation cost increases, the target grade deviation decreases dramatically; this change trend can be seen as a whole downward trend. The curve chart shows that when the transportation cost shows a small change, the grade deviation is a oscillating, not a downward trend. Therefore, this small form of change does not directly indicate the relationship between the two goals for the optimization between the total waiting time and the target grade deviation, as shown in Figure 10(d). When the total waiting time decreases, the target grade deviation rises in an oscillating trend. This change trend can be seen as an overall upward trend, but from the analysis of the curve chart, there is a small change in the total waiting time. At this time, grade deviation is a dramatic trend that does not tend downward, so this change in a small range does not directly indicate the relationship between the two goals.

The DBCDP-NSGA-II obtains a set of solutions, including the optimal solution for a single goal. In this paper, the boundary solution when each of three goals are optimal and a balanced solution for the three goals are found. The result is shown in Table 9 and compared with the value of the objective function before the optimization plan is taken. Comparing the target values of the balanced solution with the unoptimized plan, the transportation cost decreased by 18.2%, the waiting time for vehicles in queue was shortened by 55.5%, and the ore grade fluctuation declined 40.3%.

The DBCDP-NSGA-II algorithm's one-time operation results include multiple Pareto optimal solutions and multiple scheduling plans, which can meet the different production needs of the mine and provide a variety of options

TABLE 9. Multi-objective weighted objective function values.

Objective function	Transportation cost/yuan	Total waiting time/h	Grade deviation
Before optimization	41350	73.5	8.1232e-05
Equilibrium among targets	33832	32.7	4.8462e-05
Minimum shipping cost	26193	68.0	6.2724e-05
Minimum total waiting time	40068	11.5	3.5212e-05
Minimum grade deviation	34044	32.9	8.0052e-06

for open-pit mine production managers. Taking the minimum total queuing time as an example, the operating routes of 20 unmanned vehicles are shown in Table 10, and the Gantt chart of 20 unmanned vehicles is shown in Figure 11.

TABLE 10. Truck running routes.

Truck number	Running route
1	AaEbDaFbEbAaDaAaEbFaAaDbCcEbDbFbAcDbDaEcDbBbAb
2	aEbBcCbCcEaBbCaBbEcAcFcFbAbBcBaEaAaCcDcFaFbEc
3	BbFcBaEbEaBaAbAbCcDbEaBbBbEaBaBcFcDaBcDeDbCbD
4	bFbDbFaAbAcEbAcDaAcEaBcEcFcEaBaFaEbAaAcDbEcCc
5	CbBaEbFcCcCbBcCbFbCbAcBaFbDbFaCaBcEbFbDaCc
6	cBaEcCbBbCbDbAcEcDbCbFbBaBbFbEaAbEaFbBcAcEbDc
7	DbAcAaDcCbAbFaFcCbBaEaCaCaAcCcCaAaEaAaAbBcFb
8	aAbCaDaBbAbFcCcCaCbEbEaDaFcAaCaCaDbDcBaFaAaBcDcFb
9	EcBaCcDcBaFbAbAaBbCcCbAbBcDaEcCbAaDbDaCbCcAa
10	bCcCcCcAcAaBaEcEbDaDbFaCbEbDcAaCaDbDaDcEaFcDaAcBa
11	FbCcAcDcFcFaFbEbDcFaBaAbDaDaCbFbBaEaFaBbBbAcDb
12	cDcAaDaEcDcCcEeAbAaAaAcFbCaFcDbCcFaEbFcAaEcFaF
13	AbAcAbFcDaCbDcBaEbFbCbEcBaCcBaFcAbCaEbAaCaEa
14	aCcEcFaAaBbDbCaBaAaCaBcFbCcFcAcCaCcEbCcCcBbFc
15	BaFaFbCbDaAcEcCaAbBaEbAcAbCaEbCcAbCcCaFaAa
16	bAbAcFbBcCbDcEcEcDaDbBcEaFbFbAbBcBcEcEbEbDcBc
17	CcCcEbFaEaEbFaDaDcEcDbDaFbDaDcEbAcCcDcAbBaFcEb
18	cBbBbAcFcDaBaEaFbFcEaCbBcBaEaFbDaEbBaCa
19	DaAbBaEbCbFbEaEbDbCaDaAcDcBbE
20	aAbEbFcEbDaEaBbDbEaBaFaBcAbBcBaEbEbBb

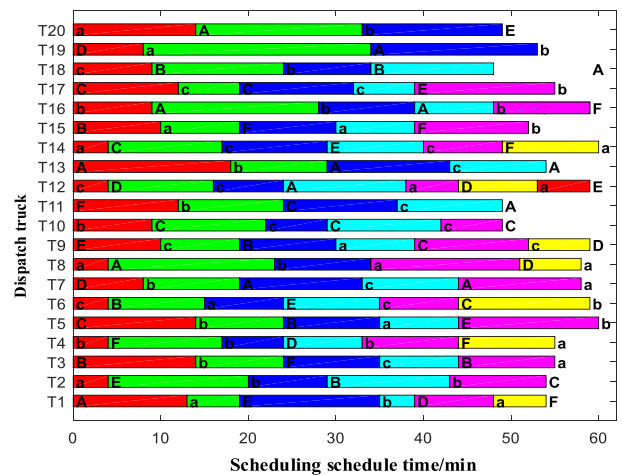


FIGURE 11. The vehicle scheduling Gantt chart.

C. INTELLIGENT TRANSPORTATION SCHEDULING SYSTEM APPLICATIONS

The system we have proposed has been applied at the Luoyang Molybdenum Sandaozhuang Open Pit Mine, which is one of the three largest molybdenum ore fields in the world; it is located in Luoyang City, Henan Province, China

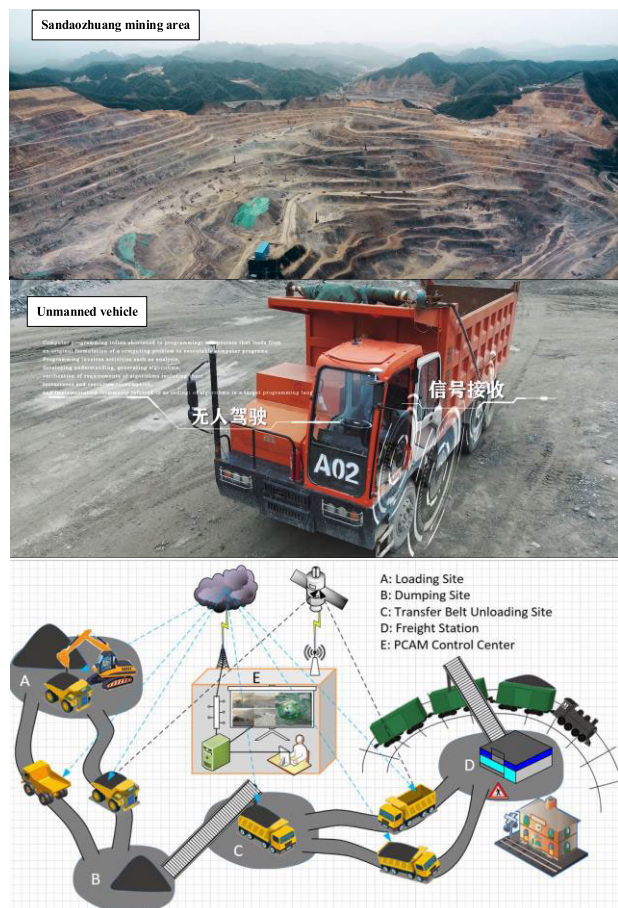


FIGURE 12. Sandaozhuang open-pit mine intelligent transportation scheduling system based on 5G and big data.

(Figure 12). The Sandaozhuang open-pit mine deployed 20 unmanned vehicles, and 5 mobile edge computing (MEC) servers for big data computing. Computing and storage resources can sync to the MEC server at the edge of the network, and the network transmission speed can also improve qualitatively. Compared with the central cloud, the MEC server is closer to the vehicle, the network transmission speed is faster, and it can cooperate with the unmanned vehicle for calculation. The MEC server can cooperate with vehicles to perform calculations by providing calculation offload services, saving vehicle energy consumption. In May 2019, the mine performed an intelligent driving trial operation of autonomous electric mining unmanned vehicles (autonomous loading, autonomous operation, autonomous reversing and autonomous unloading). In December 2019, it realized intelligent unmanned vehicles formation operation and large-scale application. After adopting the intelligent transportation scheduling system based on 5G and big data, the unmanned vehicle speed was increased from 10 km/h to 30 km/h. The system not only improves the mine's production process, it can shorten the average vehicle travel distance, increase their effective utilization rate, and achieve energy savings and consumption reduction. At the same time, it can ensure the

continuous and stable supply of mine products and increase mine benefits.

V. CONCLUSION AND FUTURE WORK

As the core content of mine production management, traditional open-pit mine truck scheduling is fraught with problems such as long waiting time for vehicles in queue and a single optimization goal. The rapid development of 5G and artificial intelligence has made open-pit mine driverless applications more and more mature. To improve the operation efficiency of traditional dispatch models, multi-objective dispatch optimization models for open-pit mine unmanned vehicles have been established. The research on algorithm solution its application in a mine was carried out. The main research conclusions are as follows:

- 1) A vehicle scheduling model for open-pit mine unmanned truck intelligent transportation systems is constructed. Based on mass data such as unmanned vehicle GPS data, vehicle equipment information, production planning data, etc., with the minimum transport cost, the smallest unmanned vehicle total queue time, and the smallest fluctuations in ore content as the objective functions, we have established an open-pit mine unmanned multi-objective intelligent vehicle dispatching model. The model simultaneously considers multiple targets to plan truck operation routes, which are aligned with actual production in open-pit mines.
- 2) Considering the advantages of the three methods of Pareto domination, decomposition and constraint domination, a decomposition and constraint domination NSGA-II optimization algorithm (DBCDDP-NSGA-II) is proposed. In the domination sorting, Pareto domination sorting is performed, and from the distance from the solution to the weight vector and the distance between the solution and the ideal point, we penalize and strictly rank the equivalent solutions in terms of the projection of the weight vector and the solution density, thereby retaining the feasible and non-feasible sparse area solutions, improving the convergence and distribution of the population. The results of this algorithm and four other algorithms for the DTLZ test function constraint are comprehensively analyzed. The simulation results show that the proposed algorithm provides the best overall performance.
- 3) The multi-objective intelligent scheduling model and solution algorithm of the open-pit mine unmanned truck proposed in this study are used in the actual scheduling of unmanned trucks in an open-pit mine intelligent mining area. Selecting the relevant data for a certain shift of a truck in the open-pit mine intelligent mining area, we use the multi-objective driverless truck intelligent scheduling model established in this paper and the proposed DBCDDP-NSGA-II optimization algorithm to obtain the pareto optimal solution set. The results of the algorithm in one run include multiple Pareto optimal solutions and multiple scheduling plans,

which can meet the different production needs of the mine and provide a variety of options for open-pit mine production managers. The results show the scheduling scheme for 20 driverless vehicles, the schedule of driverless vehicles within a shift, etc. The multi-objective optimization method of truck scheduling proposed in this paper optimizes truck scheduling in open pit mines. When applied to actual scheduling, it can reduce vehicle operating cost by 18.2%, shorten the vehicle waiting time by 55.5%, and reduce the ore content fluctuation by 40.3%.

Although our work has achieved certain results, we believe that there is room for further improvement. Firstly, there are many algorithms for solving multi-objective problems. The test sets for verifying multi-objective performance are huge. We will compare DBCDP-NSGA-II with more algorithms on more test functions. Secondly, our initial population is randomly generated. In the future, we will optimize the initial population to improve the convergence rate of the algorithm. Furthermore, open-pit mine unmanned vehicles are affected by random factors such as the environment, vehicle conditions, emergencies, etc. in the actual production scheduling process, resulting in scheduling plans that must be adjusted at various times. Adjustments need further discussion in subsequent research. In future research, the effect of dynamic time should be added to the multi-objective truck dispatching optimization model to realize the integration of real-time dispatching dynamic feedback and resource allocation scheduling. It is more practical to optimize the scheduling of unmanned vehicles in open pit mines as a whole. Finally, we hope to apply DBCDP-NSGA-II to other fields such as ship scheduling to test its ability to solve practical problems.

REFERENCES

- [1] B. Li, J. Li, K. Tang, and X. Yao, "Many-objective evolutionary algorithms: A survey," *ACM Comput. Surv.*, vol. 48, no. 1, pp. 1–35, Sep. 2015.
- [2] Y. Zeng, J. Xie, H. Jiang, G. Huang, S. Yi, N. Xiong, and J. Li, "Smart caching based on user behavior for mobile edge computing," *Inf. Sci.*, vol. 503, pp. 444–468, Nov. 2019.
- [3] J. B. Mendes, M. F. S. V. D'Angelo, N. A. Maia, and R. R. Veloso, "A hybrid multiobjective evolutionary algorithm for truck dispatching in Open-Pit-Mining," *IEEE Latin Amer. Trans.*, vol. 14, no. 3, pp. 1329–1334, Mar. 2016.
- [4] Y. Liu, A. Liu, T. Wang, X. Liu, and N. N. Xiong, "An intelligent incentive mechanism for coverage of data collection in cognitive Internet of Things," *Future Gener. Comput. Syst.*, vol. 100, pp. 701–714, Nov. 2019.
- [5] Z. Fan, W. Li, X. Cai, H. Li, C. Wei, Q. Zhang, K. Deb, and E. Goodman, "Push and pull search for solving constrained multi-objective optimization problems," *Swarm Evol. Comput.*, vol. 44, pp. 665–679, Feb. 2019.
- [6] S. Jiang, M. Lian, C. Lu, S. Ruan, Z. Wang, and B. Chen, "SVM-DS fusion based soft fault detection and diagnosis in solar water heaters," *Energy Explor. Exploitation*, vol. 37, no. 3, pp. 1125–1146, May 2019.
- [7] A. Shahzad, J.-Y. Choi, N. Xiong, Y.-G. Kim, and M. Lee, "Centralized connectivity for multiwireless edge computing and cellular platform: A smart vehicle parking system," *Wireless Commun. Mobile Comput.*, vol. 2018, pp. 1–23, 2018.
- [8] K. Gao, D. Yan, F. Yang, J. Xie, L. Liu, R. Du, and N. Xiong, "Conditional artificial potential field-based autonomous vehicle safety control with interference of lane changing in mixed traffic scenario," *Sensors*, vol. 19, no. 19, pp. 4199–4212, Sep. 2019.
- [9] W. Zhang, D. Chen, H. Si, and N. N. Xiong, "RTDCM: A coding pre-emption collection system for key data prioritization with hierarchical probability exchange mechanism in mobile computing," *IEEE Access*, vol. 8, pp. 4629–4639, 2019.
- [10] G. S. Bastos, "Decision making applied to shift change in stochastic open-pit mining truck dispatching," *IFAC Proc. Volumes*, vol. 46, no. 16, pp. 34–39, 2013.
- [11] X. Nie, S. Feng, Z. Shudu, and G. Quan, "Simulation study on the dynamic ventilation control of single head roadway in high-altitude mine based on thermal comfort," *Adv. Civil Eng.*, vol. 2019, pp. 1–12, Jul. 2019.
- [12] K. Li, K. Deb, Q. Zhang, and S. Kwong, "An evolutionary many-objective optimization algorithm based on dominance and decomposition," *IEEE Trans. Evol. Comput.*, vol. 19, no. 5, pp. 694–716, Oct. 2015.
- [13] S. Wen, C. Huang, X. Chen, J. Ma, N. Xiong, and Z. Li, "Energy-efficient and delay-aware distributed routing with cooperative transmission for Internet of Things," *J. Parallel Distrib. Comput.*, vol. 118, pp. 46–56, Aug. 2018.
- [14] K. Gao, F. Han, P. Dong, N. Xiong, and R. Du, "Connected vehicle as a mobile sensor for real time queue length at signalized intersections," *Sensors*, vol. 19, no. 9, pp. 2039–2059, Nov. 2019.
- [15] E. Topal and S. Ramazan, "A new MIP model for mine equipment scheduling by minimizing maintenance cost," *Eur. J. Oper. Res.*, vol. 207, no. 2, pp. 1065–1071, Dec. 2010.
- [16] Y. Jiang, G. Tong, H. Yin, and N. Xiong, "A pedestrian detection method based on genetic algorithm for optimize XGBoost training parameters," *IEEE Access*, vol. 7, pp. 118310–118321, 2019.
- [17] W. Gao, G. Li, Q. Zhang, Y. Luo, and Z. Wang, "Solving nonlinear equation systems by a two-phase evolutionary algorithm," *IEEE Trans. Syst., Man, Cybern. Syst.*, early access, Dec. 20, 2020.
- [18] W. Gong, Y. Wang, Z. Cai, and S. Yang, "A weighted biobjective transformation technique for locating multiple optimal solutions of nonlinear equation systems," *IEEE Trans. Evol. Comput.*, vol. 21, no. 5, pp. 697–713, Oct. 2017.
- [19] Y. R. Naidu and A. K. Ojha, "Solving multiobjective optimization problems using hybrid cooperative invasive weed optimization with multiple populations," *IEEE Trans. Syst., Man, Cybern. Syst.*, vol. 48, no. 6, pp. 821–832, Jun. 2018.
- [20] Q. Gu, H. Xie, R. R. A. Issa, and C. Lu, "Location optimization with uncertainty for industrial project using discrete block model and spatial meshing algorithm," *J. Comput. Civil Eng.*, vol. 33, no. 2, Dec. 2019, Art. no. 04018064.
- [21] G. Liu, Z. Zhuang, W. Guo, N. Xiong, and G. Chen, "A novel particle swarm optimizer with multi-stage transformation and genetic operation for VLSI routing," 2018, *arXiv:1811.10225*. [Online]. Available: <http://arxiv.org/abs/1811.10225>
- [22] J. Wang, W.-C. Yeh, N. N. Xiong, J. Wang, X. He, and C.-L. Huang, "Building an improved Internet of Things smart sensor network based on a three-phase methodology," *IEEE Access*, vol. 7, pp. 141728–141737, 2019.
- [23] S. R. Patterson, E. Kozan, and P. Hyland, "Energy efficient scheduling of open-pit coal mine trucks," *Eur. J. Oper. Res.*, vol. 262, no. 2, pp. 759–770, Oct. 2017.
- [24] P. Dong, J. Xie, W. Tang, N. Xiong, H. Zhong, and A. V. Vasilakos, "Performance evaluation of multipath TCP scheduling algorithms," *IEEE Access*, vol. 7, pp. 29818–29825, 2019.
- [25] L. Wan, L. Wei, N. Xiong, J. Yuan, and J. Xiong, "Pareto optimization for the two-agent scheduling problems with linear non-increasing deterioration based on Internet of Things," *Future Gener. Comput. Syst.*, vol. 76, pp. 293–300, Nov. 2017.
- [26] K. Zhou, J. Gui, and N. Xiong, "Improving cellular downlink throughput by multi-hop relay-assisted outband D2D communications," *EURASIP J. Wireless Commun. Netw.*, vol. 2017, no. 1, pp. 11–23, Dec. 2017.
- [27] M. Huang, A. Liu, N. N. Xiong, T. Wang, and A. V. Vasilakos, "An effective service-oriented networking management architecture for 5G-enabled Internet of Things," *Comput. Netw.*, vol. 173, May 2020, Art. no. 107208.
- [28] E. Zitzler, L. Thiele, M. Laumanns, C. M. Fonseca, and V. G. da Fonseca, "Performance assessment of multiobjective optimizers: An analysis and review," *IEEE Trans. Evol. Comput.*, vol. 7, no. 2, pp. 117–132, Apr. 2013.
- [29] J. Gui, L. Hui, and N. Xiong, "Enhancing cellular coverage quality by virtual access point and wireless power transfer," *Wireless Commun. Mobile Comput.*, vol. 2018, pp. 1–19, 2018.

- [30] H. Zheng, W. Guo, and N. Xiong, "A kernel-based compressive sensing approach for mobile data gathering in wireless sensor network systems," *IEEE Trans. Syst., Man, Cybern. Syst.*, vol. 48, no. 12, pp. 2315–2327, Dec. 2018.
- [31] V. N. Coelho, M. J. F. Souza, I. M. Coelho, F. G. Guimaraes, T. Lust, and R. C. Cruz, "Multi-objective approaches for the open-pit mining operational planning problem," *Electron. Notes Discrete Math.*, vol. 39, pp. 233–240, Dec. 2012.
- [32] M. Elarbi, S. Bechikh, A. Gupta, L. Ben Said, and Y.-S. Ong, "A new decomposition-based NSGA-II for many-objective optimization," *IEEE Trans. Syst., Man, Cybern. Syst.*, vol. 48, no. 7, pp. 1191–1210, Jul. 2018.
- [33] B. Lin, F. Zhu, J. Zhang, J. Chen, X. Chen, N. N. Xiong, and J. Lloret Mauri, "A time-driven data placement strategy for a scientific workflow combining edge computing and cloud computing," *IEEE Trans. Ind. Inform.*, vol. 15, no. 7, pp. 4254–4265, Jul. 2019.
- [34] H. Li and Q. Zhang, "Multiobjective optimization problems with complicated Pareto sets, MOEA/D and NSGA-II," *IEEE Trans. Evol. Comput.*, vol. 13, no. 2, pp. 284–302, Apr. 2009.
- [35] S. Jiang, C. Lu, S. Zhang, X. Lu, S.-B. Tsai, C.-K. Wang, Y. Gao, Y. Shi, and C.-H. Lee, "Prediction of ecological pressure on resource-based cities based on an RBF neural network optimized by an improved ABC algorithm," *IEEE Access*, vol. 7, pp. 47423–47436, 2019.
- [36] G. Du, G. Tong, and N. Xiong, "An individual and model-based offspring generation strategy for evolutionary multiobjective optimization," *IEEE Access*, vol. 7, pp. 34675–34686, 2019.
- [37] H. Teng, Y. Liu, A. Liu, N. N. Xiong, Z. Cai, T. Wang, and X. Liu, "A novel code data dissemination scheme for Internet of Things through mobile vehicle of smart cities," *Future Gener. Comput. Syst.*, vol. 94, pp. 351–367, May 2019.
- [38] E. S. Matrosov, I. Huskova, J. R. Kasprzyk, and J. J. Harou, "Many-objective optimization and visual analytics reveal key trade-offs for London's water supply," *J. Hydrol.*, vol. 15, no. 18, pp. 1040–1053, Dec. 2015.
- [39] C. von Lüken, B. Barán, and C. Brizuela, "A survey on multi-objective evolutionary algorithms for many-objective problems," *Comput. Optim. Appl.*, vol. 58, pp. 707–756, Feb. 2014.
- [40] W. Fang, S. Ding, Y. Li, W. Zhou, and N. Xiong, "OKRA: Optimal task and resource allocation for energy minimization in mobile edge computing systems," *Wireless Netw.*, vol. 25, no. 5, pp. 2851–2867, Jul. 2019.
- [41] Q. Gu, X. Li, and S. Jiang, "Hybrid genetic grey wolf algorithm for large-scale global optimization," *Complexity*, vol. 2019, pp. 1–18, Feb. 2019.
- [42] Y. Fang, Q. Chen, N. N. Xiong, D. Zhao, and J. Wang, "RGCA: A reliable gpu cluster architecture for large-scale Internet of Things computing based on effective performance-energy optimization," *Sensors*, vol. 17, no. 8, pp. 11–23, Jun. 2017.
- [43] S. Ruan, H. Xie, and S. Jiang, "Integrated proactive control model for energy efficiency processes in facilities management: Applying dynamic exponential smoothing optimization," *Sustainability*, vol. 9, no. 9, pp. 1597–1610, Sep. 2017.
- [44] X. Chen, G. Liu, N. Xiong, Y. Su, and G. Chen, "A survey of swarm intelligence techniques in VLSI routing problems," *IEEE Access*, vol. 8, pp. 26266–26292, 2020.



CAIWU LU received the B.S. degree from the Department of Mining, Xi'an University of Architecture and Technology, Shaanxi, China, in 1987, and the Ph.D. degree in mine engineering from Northeastern University, Shenyang, China, in 1998. He is currently a Professor with the School of Management and School of Resources Engineering, Xi'an University of Architecture and Technology, Shaanxi. His research interest fields in mining system engineering, including mining management and optimization related production, dispatching, ore blending, and intelligent mining. He is the author of five books, more than 100 articles, and more than 20 inventions.



SONG JIANG received the M.S. degree in mine engineering from the School of Management, Xi'an University of Architecture and Technology, Shaanxi, China, in 2012, where he is currently pursuing the Ph.D. degree. He is the author of two books and more than 20 articles. His research interests include mining system engineering, big data, and mining management. He has a strong interest in the exploration of interdisciplinary fields of computers and mine.



LU SHAN received the B.S. degree in economics from the University of California, Los Angeles. She is currently pursuing the master's degree in economics with The Hong Kong University of Science and Technology. She had previously worked at the Morgan Stanley Wealth Management. She studies macro-finance models of asset pricing and investment with financial frictions, and has strong interests in interdisciplinary cooperation with bionic optimizations and its applications in economics.



NEAL NAIXUE XIONG (Senior Member, IEEE) received the Ph.D. degrees from Wuhan University, in 2007, about sensor system engineering, and from the Japan Advanced Institute of Science and Technology, in 2008, about dependable communication networks, respectively. He is currently an Associate Professor (5rd year) with the Department of Mathematics and Computer Science, Northeastern State University, OK, USA. Before he attended Northeastern State University, he worked in Georgia State University, Wentworth Technology Institution, and Colorado Technical University (full professor about five years) about 10 years. He has published over 200 international journal articles and over 100 international conference papers. Some of his works were published in the IEEE JOURNAL ON SELECTED AREAS IN COMMUNICATIONS, IEEE or ACM transactions, ACM Sigcomm workshop, IEEE INFOCOM, ICDCS, and IPDPS. His research interests include cloud computing, security and dependability, parallel and distributed computing, networks, and optimization theory.

Dr. Xiong has received the Best Paper Award in the 10th IEEE International Conference on High Performance Computing and Communications (HPCC-08) and the Best student Paper Award in the 28th North American Fuzzy Information Processing Society Annual Conference (NAFIPS2009). He has been a General Chair, Program Chair, Publicity Chair, Program Committee member, and Organizing Committee member of over 100 international conferences, and as a reviewer of about 100 international journals, including the IEEE JOURNAL ON SELECTED AREAS IN COMMUNICATIONS, IEEE SMC (Park: A/B/C), the IEEE TRANSACTIONS ON COMMUNICATIONS, IEEE TRANSACTIONS ON MOBILE COMPUTING, and IEEE TRANSACTIONS ON PARALLEL AND DISTRIBUTED SYSTEMS. He is serving as an Editor-in-Chief, an Associate Editor or an Editor member for over ten international journals (including an Associate Editor of the IEEE TRANSACTIONS ON SYSTEMS, MAN AND CYBERNETICS: SYSTEMS, an Associate Editor of *Information Science*, an Editor-in-Chief of *Journal of Internet Technology* (JIT), and an Editor-in-Chief of *Journal of Parallel and Cloud Computing* (PCC), and a Guest Editor for over ten international journals, including *Sensor Journal*, WINET, and MONET.



SAI ZHANG received the B.S. degree from the School of Resources Engineering, Shaanxi University of Science and Technology, Shaanxi, China, in 2012. He is currently pursuing the Ph.D. degree with the School of Management, Xi'an University of Architecture and Technology, Shaanxi. His research interests include information fusion, multi-objective optimization, and mining system engineering. He has a strong interest in the exploration of interdisciplinary fields of computers and mine.